nature photonics

LETTERS

PUBLISHED ONLINE: 11 JULY 2010 | DOI: 10.1038/NPHOTON.2010.165

Broadband terahertz wave remote sensing using coherent manipulation of fluorescence from asymmetrically ionized gases

Jingle Liu[1], Jianming Dai[1], See Leang Chin[2] and X.-C. Zhang[1]*

Terahertz wave sensing and imaging have received a great deal of attention because of their significant scientific and technological potential in multidisciplinary fields[1–3]. However, owing to the challenge of dealing with high ambient moisture absorption, the development of remote open-air broadband terahertz spectroscopy is lagging behind the urgent need for the technology that exists in homeland security and the fields of astronomy and environmental monitoring[3,4]. The requirement for on-site bias or forward collection of the optical signal in conventional terahertz detection techniques has inevitably prohibited their use in remote sensing[5–7]. We introduce an 'all-optical' technique of broadband terahertz wave detection by coherently manipulating the fluorescence emission from asymmetrically ionized gas plasma interacting with terahertz waves. Owing to the high atmospheric transparency and omnidirectional emission pattern of the fluorescence, this technique can be used to measure terahertz pulses at standoff distances with minimal water vapour absorption and unlimited directionality for optical signal collection. We demonstrate coherent terahertz wave detection at a distance of 10 m.

Photoconductive antennas[5], electro-optic (EO) sampling[6] and terahertz air detection[7] have been widely used in recent decades for the detection of broadband terahertz radiation in an increasing variety of applications including biomedical imaging, non-destructive inspection and material characterization[1–3]. In attempts to meet the emerging needs of homeland security and environmental science, a large amount of research effort has been directed at developing broadband remote terahertz spectroscopy. Focusing two-colour optical beams remotely provides a solution for remote terahertz wave generation[8]. However, the realization of broadband terahertz remote sensing is even more challenging because of the strong absorption of ambient water vapour in the terahertz band and the difficulties inherent to remote optical signal collection. Using a biased photoconductive antenna[5] or EO crystal[6] for terahertz-wave remote sensing is not practical. In terahertz wave detection using a gas sensor[7], the second-harmonic beam, generated from a four-wave-mixing process involving the terahertz beam and the fundamental laser beam, has to be measured in the forward direction, so collecting it is difficult at standoff distances due to weak scattering.

Here, we report on an 'all-optical' technique for standoff (10-m) broadband coherent terahertz wave detection by probing the terahertz pulse with a fully controllable two-colour laser-induced gas plasma and analysing the interaction by detecting the omnidirectional fluorescence emission. The high transparency of UV fluorescence in the atmosphere can circumvent the sensing distance limitation that arises due to strong water vapour absorption in the terahertz region. Instead of being used for terahertz wave generation as demonstrated in ref. 9, the two-colour laser field functions as a remote 'optical modulator' for the terahertz radiation enhanced emission of fluorescence (THz-REEF) signal through coherent manipulation of the ionized electron drift velocity and subsequent collision-induced fluorescence emission. We will further reveal the complex physical picture of the light–plasma interaction by investigating the relation between the fluorescence and the electron momentum distribution. THz-REEF from gas plasma excited by single-colour, multicycle laser pulses has been studied and demonstrated for terahertz wave detection[10]. However, this method only detects terahertz wave intensity, and not phase information, which makes it non-ideal for remote sensing due to the requirement for an on-site external electric bias to provide a local oscillator. Unlike the inherently incoherent scheme in ref. 10, this technique using symmetry-broken laser fields to control electron momentum is inherently coherent and directly measures the terahertz field $E_{\mathrm{THz}}(t)$ instead of the vector potential $A_{\mathrm{THz}}(t)$. The performance of this technique regarding terahertz wave detection is one to two orders better than that using bias as in ref. 10 due to the larger modulation of the electron momentum and elimination of noise induced by the derivative relation $E_{\mathrm{THz}}(t) = \mathrm{d}A_{\mathrm{THz}}(t)/\mathrm{d}t$. Furthermore, this technique circumvents the limitations of the on-site bias requirement, water vapour attenuation and signal-collection direction at standoff distances. By applying this technique we have realized the detection of broadband terahertz radiation from a distance of 10 m.

Figure 1 presents a schematic of experiments on terahertz wave remote sensing, using coherent manipulation of terahertz wave enhanced fluorescence from asymmetrically ionized gas. The two-colour laser beam with parallel polarization was focused into air to generate plasma, with the relative phase being controlled by an in-line phase compensator[9]. A single-cycle terahertz pulse with a peak field of 100 kV cm^{-1} was focused collinearly with the optical beam onto the plasma. The shaded area in Fig. 1 shows the fluorescence detection system, which has translational mobility on a horizontal plane. The fluorescence emitted from the two-colour laser-induced plasma was collected by a rotatable UV-enhanced concave mirror (M1) with a diameter of 200 mm and focal length of 500 mm, and was then guided by another UV plane mirror (M2) with a diameter of 75 mm through a monochromator into a photomultiplier tube (PMT). Terahertz wave sensing was performed as the distance between the plasma and fluorescence detection system was varied.

In the laser-induced ionization processes, electrons newly released from molecules or atoms acquire a constant drift velocity after passage of the laser pulse[11]. The drift velocity is determined

[1]Center for Terahertz Research, Rensselaer Polytechnic Institute, Troy, New York 12180, USA, [2]Department of Physics, Center for Optics, Photonics and Laser, Laval University, Quebec City, Quebec, G1V 0A6, Canada. *e-mail: zhangxc@rpi.edu

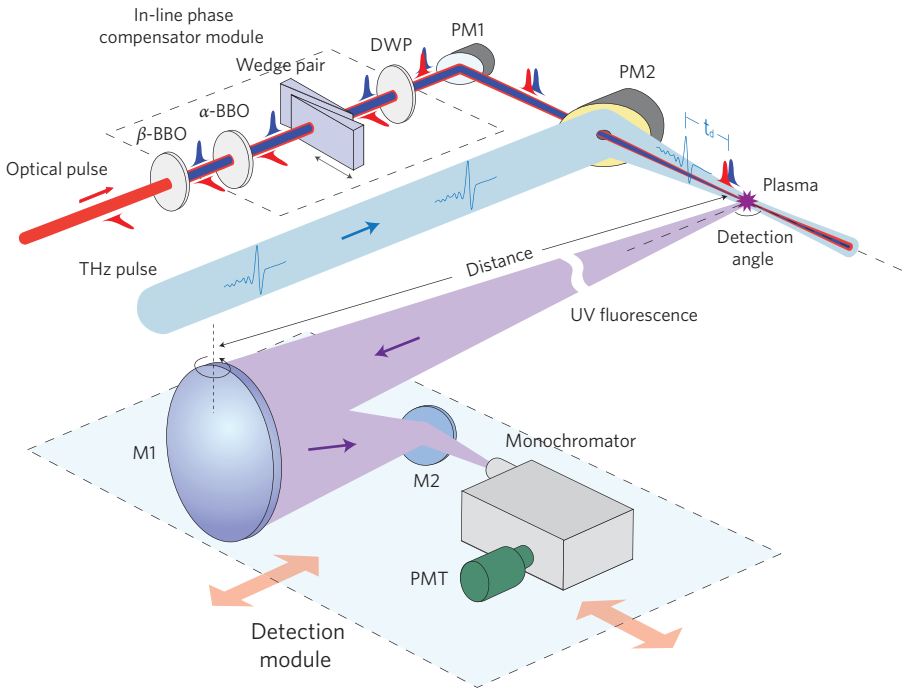

Figure 1 | Schematic of the terahertz wave remote sensing technique. The 2ω pulse is generated by passing the fundamental beam through a type I β-BBO crystal. Both the fundamental and second-harmonic optical pulses are linearly polarized along a vertical direction. The relative phase change between the ω and 2ω pulses is tuned by the lateral translation of fused silica wedges in the optical beam path after the α-BBO. The two optical pulses are focused by a parabolic mirror (effective focal length, 150 mm) into air to generate plasma. The time delay t_d is defined as the delay between the optical pulse peak and terahertz pulse peak. The fluorescence detection system consists of a UV concave mirror (M1; diameter, 200 mm and focal length, 500 mm), a UV plane mirror (M2), a monochromator and a photomultiplier tube (PMT). The distance of remote sensing is varied by moving the fluorescence detection system with respect to the plasma. DWP, dual-band waveplate.

by the phase of the laser field at the birth of the free electron. Residual current density or asymmetric electron velocity distribution could remain in the plasma, ionized by single-colour few-cycle pulses[12] or by two-colour fields with optimized relative phase[13,14]. Under irradiation from intense laser pulses, some of the excited electrons are trapped in high-lying states of atoms and molecules[15–18]. Those trapped states have a large principal quantum number ($n \gg 1$) and are more easily ionized by collision with energetic electrons[19–21], as illustrated in Fig. 2a. The interaction of laser-induced plasma with a terahertz wave leads to an increase in plasma temperature through electron acceleration. Electron impact produces more ionized gas species and subsequently generates more $N_2(C^3\Pi_\pi)$ through dissociative recombination[22]. In single-colour, multicycle laser pulse excitation, which results in a symmetric electron drift velocity distribution, THz-REEF from nitrogen plasma is quadratically dependent on the terahertz field[10]. Similar phenomena were also observed in argon, krypton and xenon gas plasmas.

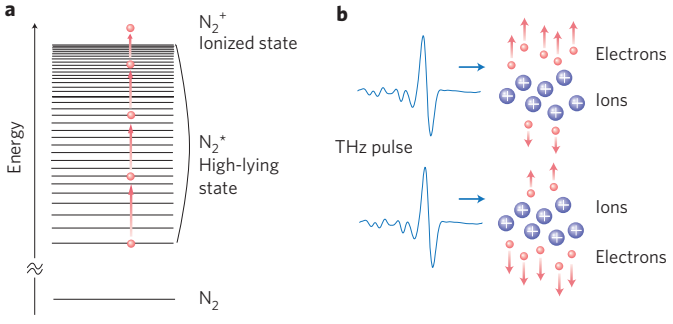

Figure 2 | The terahertz wave assisted electron impact ionization of high-lying states in plasma. a, High-lying states can be ionized by a series of collisions with energetic electrons. **b**, Interaction between the terahertz pulse and the asymmetric photoelectron velocity distributions generated by two-colour field ionization.

Contrarily, the synthesized optical field of two-colour pulses generates ionized electrons with an asymmetric drift velocity. The drift velocity distribution and electron trajectories can be controlled by the polarizations and relative phase of two optical fields $\phi_{\omega,2\omega}$ (refs 9,23). After the passage of two-colour pulses, the electric field of a single-cycle terahertz pulse applied to the laser-induced plasma alters the ionized electron momentum by acceleration or deceleration, depending on the electron initial velocity $\mathbf{v}(0)$ (see Fig. 2b). Because both the amplitude and direction of the terahertz field affect plasma fluorescence, the terahertz waveform information is encoded into a change of fluorescence at a different time delay t_d between the terahertz pulse and the optical pulses. We demonstrate that a terahertz waveform can be retrieved by measuring time-dependent fluorescence emission when $\mathbf{v}(0)$ is aligned both parallel and antiparallel to $\mathbf{E}_{THz}(t)$.

Fluorescence intensities at different $\Delta\phi_{\omega,2\omega}$ were recorded as the time delay t_d between the external terahertz pulse and the two overlapping optical pulses was changed. The sliced, individual, time-delay-dependent THz-REEF $\Delta I_{FL}(t_d, \pm(2l+1)\pi/2)$ for the same external terahertz pulse and optical intensity is presented in Fig. 3a. The ionized electron velocity distribution $\rho(\mathbf{v}(0), \Delta\phi_{\omega,2\omega})$ is strongly asymmetric at the phase generating the largest photocurrent (relative phase change $\Delta\phi_{\omega,2\omega} = \pm(2l+1)\pi/2$), but almost symmetric at the phase generating the smallest photocurrent ($\Delta\phi_{\omega,2\omega} = \pm l\pi$) (refs 13,24). The different shapes of $\Delta I_{FL}(t_d, \Delta\phi_{\omega,2\omega})$ indicate how the initial electron drift velocity distribution $\rho(\mathbf{v}_e, \Delta\phi_{\omega,2\omega})$ affects electron heating by the terahertz field and

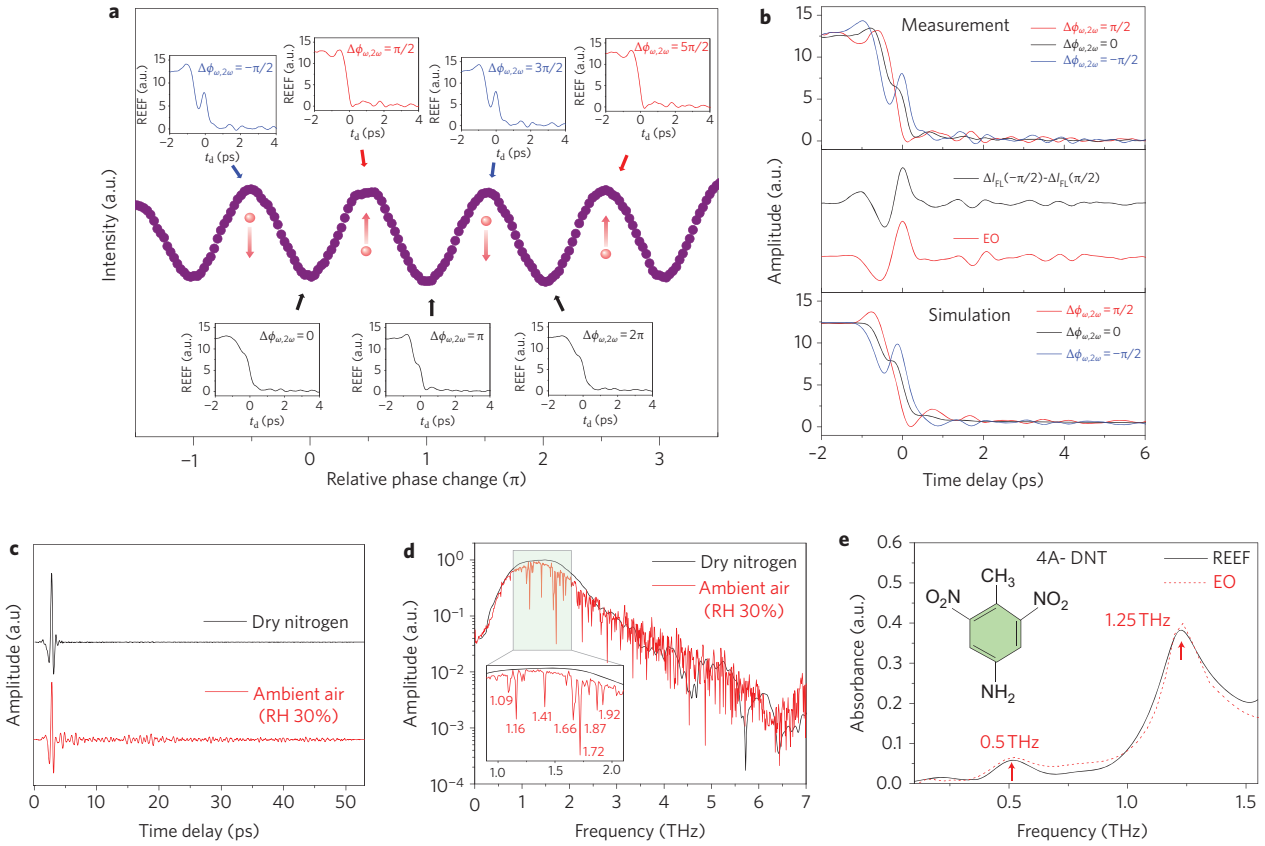

Figure 3 | Differential THz-REEF, coherent terahertz detection and simulation. a, Measured time-dependent REEF at a relative optical phase change of $\Delta\phi_{\omega,2\omega} = \pm/\pi/2$. The terahertz wave enhanced fluorescence shows significant dependence on the initial electron velocity distribution, which is determined by $\Delta\phi_{\omega,2\omega}$. **b**, Top: measured THz-REEF at phase $\Delta\phi_{\omega,2\omega} = 0, \pm\pi/2$, respectively. The symmetry of the red and blue lines with respect to the black line arises from opposite electron velocity distributions at $\pm\pi/2$ as the terahertz field direction remains unchanged. Middle: comparison of the terahertz waveform measured by EO sampling and the terahertz waveform obtained from the difference of the two REEF curves with opposite velocity distributions. Bottom: simulated THz-REEF derived from equation (2) at $\Delta\phi_{\omega,2\omega} = 0, \pm\pi/2$. **c**, Measured terahertz waveforms using REEF in dry nitrogen or in an ambient air environment. **d**, Corresponding terahertz spectra in a logarithmic scale. Spectral resolution, 0.02 THz. Inset: enlarged view of water vapour absorption features in the shaded area of the main panel. **e**, Comparison of terahertz absorption spectra of 4A-DNT measured by REEF and that measured with EO sampling. RH, relative humidity.

energy transfer in the electron–molecule inelastic collision. $\Delta I_{FL}(t_d,\pi/2)$ and $\Delta I_{FL}(t_d,-\pi/2)$ are found to be symmetric around $\Delta I_{FL}(t_d,0)$, as shown in Fig. 3b (top).

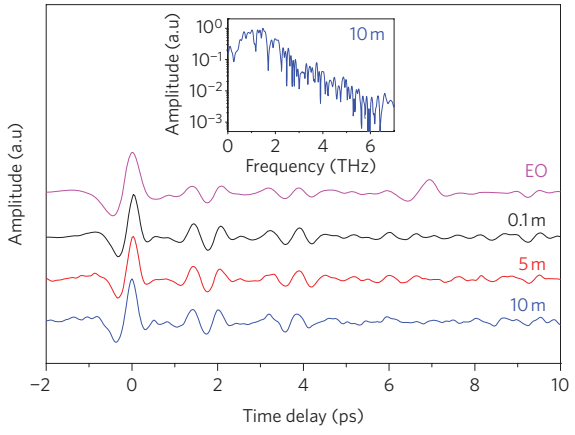

Figure 4 | Broadband terahertz wave remote sensing. Terahertz waveforms measured by EO sampling and REEF at different distances from the plasma. The waveforms are normalized and shifted for clarity. Inset: terahertz spectrum measured at a distance of 10 m.

Information about the time-dependent terahertz field can be directly retrieved by taking the differential between $\Delta I_{FL}(\Delta\phi_{\omega,2\omega} = \pi/2)$ and $\Delta I_{FL}(\Delta\phi_{\omega,2\omega} = -\pi/2)$. The terahertz waveform obtained by differentiation was compared to the terahertz waveform measured with a 300-μm ⟨110⟩ GaP crystal by EO sampling[6], as shown in Fig. 3b (middle). Using the semiclassical model, we simulated THz-REEF at different phases by calculating the interaction between the terahertz pulse shown in Fig. 3b (bottom) and two-colour ionized plasma. The calculated phase dependence agrees well with the measurements and provides a descriptive framework underpinning the primary experimental observation.

To demonstrate its capability in broadband, high-resolution, terahertz time-domain spectroscopy, THz-REEF was used to measure terahertz waveforms in ambient air and a relative humidity of 30% (Fig. 3c). An oscillatory feature after the main peaks due to water vapour absorption is clearly shown in the measured terahertz waveform in ambient air when compared with a reference waveform measured when the entire optical system except the fluorescence detection module was purged with dry nitrogen gas. Figure 3d plots the corresponding spectra, in which sharp absorption lines of water molecules can be well resolved, these line positions being consistent with previous measurement results[25]. We also measured the absorption spectrum of a 4-amino-2,6-dinitrotoluene (4A-DNT) pellet sample and compared this with the results obtained using

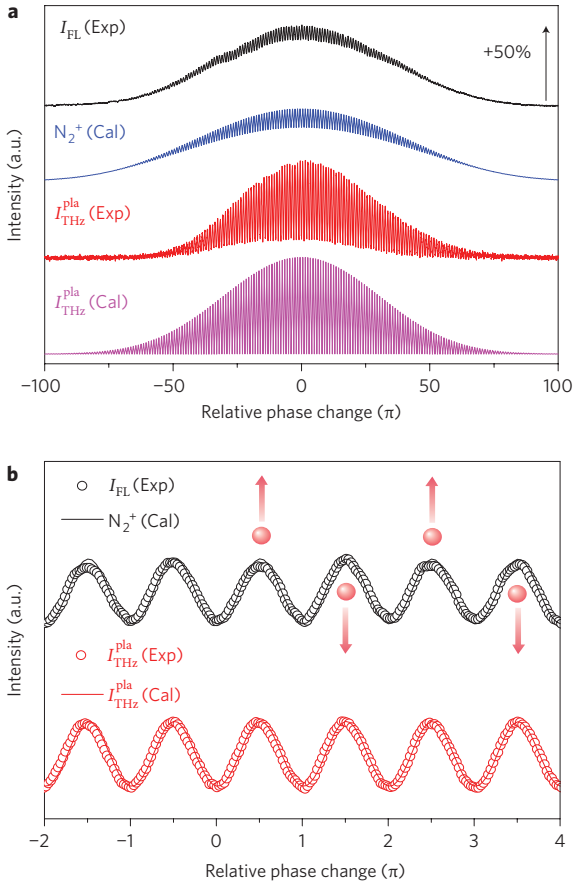

Figure 5 | Two-colour phase dependence of fluorescence and terahertz wave emission. a, Comparison of the measured phase dependence of fluorescence emission I_{FL} and plasma-photocurrent-induced terahertz emission I_{THz}^{pla} with the calculated phase dependence of ion yield N_2^+ and I_{THz}^{pla}. **b**, Enlarged view of **a** (shifted and normalized for clarity). Electron velocity direction is reversed as $\Delta\phi_{\omega,2\omega}$ is changed by π. Exp, experimental; Cal, calculated.

EO sampling. The transmission spectroscopic results measured by the two methods (plotted in Fig. 3e) show good agreement.

The standoff terahertz wave sensing capability of this method was tested by measuring the terahertz waveform carried by UV fluorescence (357 nm) when the fluorescence detection system was placed at distances of 0.1, 5 and 10 m away from terahertz source/plasma at a detection angle of 90°. Figure 4 shows that the waveforms measured by REEF are consistent with that measured by EO. Despite the decreased fluorescence collection efficiency and the reduced signal-to-noise ratio as the distance increases, the remote sensing system can clearly resolve the terahertz spectrum at a distance of 10 m. The water vapour absorption present in the spectrum is due to the short-distance (~30 cm) propagation of the terahertz wave from the local terahertz source to the plasma.

In conclusion, we have introduced a technique for standoff terahertz wave detection using the intrinsic physical properties of THz-REEF from two-colour laser-induced gas plasma. The time-dependent THz-REEF can be modified by changing the relative phase of the two-colour fields and their polarizations, providing a unique approach to detecting the amplitude and phase of terahertz waves. With its omnidirectional emission pattern and minimal ambient water vapour absorption, this technique, together with the previously demonstrated long-distance terahertz wave generation, makes broadband standoff terahertz spectroscopy feasible[8,26].

Methods

Experimental details. The THz-REEF experiment with gas plasma excited by two-colour laser fields, superposition of a linearly polarized fundamental pulse E_ω and its second-harmonic pulse $E_{2\omega}$ was created by propagating a 80-fs, 100-μJ, 800-nm laser pulse through a 250-μm type-I beta-barium borate (β-BBO). The relative phase, $\phi_{\omega,2\omega}$, was controlled by an in-line phase compensator consisting of an alpha-barium borate (α-BBO) time plate, a pair of fused silica wedges, and a dual wavelength plate (DWP, Alphalas GmbH), with attosecond phase-control accuracy[9]. The two-colour laser beam was focused into air to generate plasma. The two optical intensities at the focus were I_ω ($\sim 10^{13} - 10^{14}$ W cm^{-2}) for the fundamental beam, and $I_{2\omega}$ ($=I_\omega/10$) for the second-harmonic beam, respectively. The E_ω direction could be changed by rotating the DWP while keeping the $E_{2\omega}$ direction unchanged. To create an asymmetric electron drift velocity, E_ω and $E_{2\omega}$ were aligned parallel. The synthesized optical field E_{Opt} can be expressed as

$$E_{Opt}(t) = E_\omega(t) + E_{2\omega}(t) = A_{\omega 0}(t)\cos(\omega t) + A_{2\omega 0}(t)\cos(2\omega t + \phi_{\omega,2\omega}) \quad (1)$$

Where $A_{\omega 0}(t)$ and $A_{2\omega 0}(t)$ are the envelopes of fundamental (frequency ω) and second-harmonic (frequency 2ω) pulses, respectively. For the conceptual demonstration of terahertz wave remote sensing, a single-cycle terahertz pulse $\mathbf{E}_{THz}(t)$ with a peak field of 100 kV cm^{-1} was generated locally from a $LiNbO_3$ prism using an optical pulse with a tilted pulse front as the excitation[27] and was focused collinearly with the optical beam onto the plasma.

Two-colour phase dependence of electron velocity distribution. The phase dependence of the ionized electron velocity distribution was measured by monitoring the intensity of the plasma-photocurrent-induced terahertz wave emission, I_{THz}^{pla} and the fluorescence intensity radiated from the two-colour excited plasma, I_{FL}. In this measurement, the external terahertz pulse from $LiNbO_3$ was blocked to eliminate any interaction between the plasma and other terahertz sources. I_{THz}^{pla} was measured using a pyroelectric detector in the forward direction after filtering out the ω and 2ω pulses. I_{FL} was measured by a monochromator and the photomultiple tube (PMT), as shown in Fig. 1. The monochromator was set to pass through only the strongest molecular nitrogen emission line at 357 nm. When two optical pulses were overlapped and interfered with one another in the time domain, the fluorescence emission was enhanced by 50% compared to that generated by two temporally separated pulses. Figure 5a shows the measurement results in comparison with the numerically calculated phase dependences of I_{THz}^{pla} and total ion yield N_2^+ by using the general Ammosov–Delone–Krainov (ADK) tunnelling ionization model[28] and tracing the ionized electron motion[14]. For the intensity regime of interest here, both the measured and calculated results show that I_{THz}^{pla} and the N_2^+ yield have the same periodic dependence on the relative phase change $\Delta\phi_{\omega,2\omega}$ (Fig. 5b). The velocity distribution is a periodic function; that is, $\rho(\mathbf{v}(0), \Delta\phi_{\omega,2\omega}) = \rho(-\mathbf{v}(0), \Delta\phi_{\omega,2\omega} + \pi)$. The ionized electron velocity distribution $\rho(\mathbf{v}(0), \Delta\phi_{\omega,2\omega})$ is strongly asymmetric at the phase generating the largest photocurrent ($\Delta\phi_{\omega,2\omega} = \pm(2l+1)\pi/2$ in Fig. 5b) but almost symmetric at the phase generating the smallest photocurrent ($\Delta\phi_{\omega,2\omega} = \pm l\pi$ in Fig. 5b)[13,24].

Calculation of two-colour phase dependence of REEF. To interpret the observed phase dependence of ΔI_{FL}, we used the semiclassical scenario of electron heating by a terahertz wave, electron–molecule energy transfer and ionization of the high-lying states. Because the electron mass m_e is much smaller than the molecular mass, the average energy transferred from electrons to molecules in each collision is $(2m_e/M)m_e\mathbf{v}_i^2/2$ and is of the order of meV at an electron temperature of 1×10^5 K (ref. 29). Owing to the quasi-continuum nature of the spectra of the high-lying states, those states can be promoted 'incrementally' by many collisions until they are ionized. The total enhanced fluorescence emission due to energy transfer in a long time limit can be expressed as

$$\Delta I_{FL}(\Delta\phi_{\omega,2\omega}) \propto n_e\left[\int_{-\infty}^{+\infty}(m_e\mathbf{v}^2(0) + 2m_e\mathbf{v}(0)\Delta\mathbf{v}_1) \times \rho(\mathbf{v}(0), \Delta\phi_{\omega,2\omega})d\mathbf{v}(0)/2 + m_e\sum_{i=1}^{\infty}\Delta\mathbf{v}_i^2\right] \quad (2)$$

where n_e is the electron density and $\Delta\mathbf{v}_i = -\int_{t_i-\tau}^{t_i} e\mathbf{E}_{THz}(t)dt/m_e$. The $m_e\mathbf{v}^2(0)$ term is the energy transferred from the initial electron kinetic energy depending on laser intensity. The $\mathbf{E}_{THz}$ first-order term, $2m_e\mathbf{v}(0)\Delta\mathbf{v}_1$, originates from acceleration before the first collision. The $\mathbf{E}_{THz}$ second-order term, $m_e\sum_{i=1}^{\infty}\Delta\mathbf{v}_i^2$, is the energy transferred from the external terahertz field. Applying the symmetry $\rho(\mathbf{v}_e, \pi/2) = \rho(-\mathbf{v}_e, -\pi/2)$ to equation (2) gives

$$\Delta I_{FL}(\Delta\phi_{\omega,2\omega} = \pi/2) - \Delta I_{FL}(\Delta\phi_{\omega,2\omega} = 0) = -[\Delta I_{FL}(\Delta\phi_{\omega,2\omega} = -\pi/2) - \Delta I_{FL}(\Delta\phi_{\omega,2\omega} = 0)]$$

As electron relaxation time τ (~350 fs; ref. 30) at atmospheric pressure is small compared to the terahertz pulse cycle (~1.5 ps), the terahertz field can be considered nearly constant between neighbouring collisions. The information about the time-dependent terahertz field can be directly retrieved by taking the differential between $\Delta I_{FL}(\Delta\phi_{\omega,2\omega} = \pi/2)$ and $\Delta I_{FL}(\Delta\phi_{\omega,2\omega} = -\pi/2)$:

$$\Delta I_{FL}(\Delta\phi_{\omega,2\omega} = -\pi/2) - \Delta I_{FL}(\Delta\phi_{\omega,2\omega} = \pi/2) \propto n_e\rho(\mathbf{v}_e, 0)e\tau\mathbf{v}_e(0)\mathbf{E}_{THz} \propto \mathbf{E}_{THz} \quad (3)$$

Sample preparation. The 4A-DNT sample used in terahertz spectroscopy was a 0.5-mm-thick pellet consisting of 20% 4A-DNT and 80% polyethylene. All the sample constituents were gently ground to powder and compressed into a pellet using 5 tons of pressure from a hydraulic press. The sample was placed in the path of the terahertz beam before the parabolic mirror focusing the terahertz beam.

Received 8 December 2009; accepted 6 May 2010; published online 11 July 2010

References

1. Ferguson, B. & Zhang, X.-C. Materials for terahertz science and technology. *Nature Mater.* **1,** 26–33 (2002).
2. Mittleman, D. *Sensing with Terahertz Radiation* (Springer, 2003).
3. Tonouchi, M., Cutting-edge terahertz technology. *Nature Photon.* **1,** 97–105 (2007).
4. Federici, J. F. *et al.* THz imaging and sensing for security applications—explosives, weapons and drugs. *Semicond. Sci. Technol.* **20,** S266–S280 (2005).
5. Exter, M. V., Fattinger, Ch. & Grischkowsky, D. High-brightness terahertz beams characterized with an ultrafast detector. *Appl. Phys. Lett.* **55,** 337–339 (1989).
6. Wu, Q. & Zhang, X.-C. Free-space electro-optic sampling of terahertz beams. *Appl. Phys. Lett.* **67,** 3523–3525 (1995).
7. Dai, J., Xie, X. & Zhang, X.-C. Detection of broadband terahertz waves with a laser-induced plasma in gases. *Phys. Rev. Lett.* **97,** 103903 (2006).
8. Dai, J., Liu, J. & Zhang, X.-C. Terahertz wave air photonics: terahertz wave generation and detection with laser-induced gas plasma. *IEEE J. Sel. Topics Quantum Electron.* (in the press).
9. Dai, J., Karpowicz, N. & Zhang, X.-C. Coherent polarization control of terahertz waves generated from two-color laser-induced gas plasma. *Phys. Rev. Lett.* **103,** 023001 (2009).
10. Liu, J. & Zhang, X.-C. Terahertz radiation enhanced emission of fluorescence from gas plasma. *Phys. Rev. Lett.* **103,** 235002 (2009).
11. Corkum, P. B., Burnett, N. H. & Brunel, F. Above-threshold ionization in the long-wavelength limit. *Phys. Rev. Lett.* **62,** 1259–1262 (1989).
12. Kresβ M. *et al.* Determination of the carrier-envelope phase of few-cycle laser pulses with terahertz-emission spectroscopy. *Nature Phys.* **2,** 327–331 (2006).
13. Schumacher, D. W., Weihe, F., Muller, H. G. & Bucksbaum, P. H. Phase dependence of intense field ionization: a study using two colors. *Phys. Rev. Lett.* **73,** 1344–1347 (1994).
14. Kim, K. Y., Taylor, A. J., Glownia, J. H. & Rordriguez, G. Coherent control of terahertz supercontinuum generation in ultrafast laser–gas interactions. *Nature Photon.* **2,** 605–609 (2008).
15. Kulander, K. C., Schafer, K. J. & Krause, J. L. Dynamic stabilization of hydrogen in an intense, high-frequency, pulsed laser field. *Phys. Rev. Lett.* **66,** 2601–2604 (1991).
16. Fedorov, M. V. *Progress in Ultrafast Intense Laser Science* Vol. I (Springer, 2006).
17. Talebpour, A., Liang, Y. & Chin, S. L. Population trapping in the CO molecule. *J. Phys. B* **29,** 3435–3442 (1996).
18. Talebpour, A., Chien, C. Y. & Chin, S. L. Population trapping in rare gases. *J. Phys. B* **29,** 5725–5733 (1996).
19. Azarm, A. *et al.* Direct observation of super-excited states in methane created by a femtosecond intense laser field. *J. Phys. B* **41,** 225601 (2008).
20. Phelps, A. V. Rotational and vibrational excitation of molecules by low-energy electrons. *Rev. Mod. Phys.* **40,** 399–410 (1968).
21. Filin, A., Compton, R., Romanov, D. A. & Levis, R. J. Impact-ionization cooling in laser-induced plasma filaments. *Phys. Rev. Lett.* **102,** 155004 (2009).
22. Xu, H. L., Azarm, A., Bernhardt, J., Kamali, Y. & Chin, S. L. The mechanism of nitrogen fluorescence inside a femtosecond laser filament in air. *Chem. Phys.* **360,** 171–175 (2009).
23. Wen, H. & Lindenberg, A. M. Coherent terahertz polarization control through manipulation of electron trajectories. *Phys. Rev. Lett.* **103,** 023902 (2009).
24. Karpowicz, N. & Zhang, X.-C. Coherent terahertz echo of tunnel ionization in gases. *Phys. Rev. Lett.* **102,** 093001 (2009).
25. Exter, M. V., Fattinger, Ch. & Grischkowsky, D. Terahertz time-domain spectroscopy of water vapor. *Opt. Lett.* **14,** 1128–1130 (1989).
26. Dai, J. & Zhang, X.-C. Terahertz wave generation from gas plasma using a phase compensator with attosecond phase-control accuracy. *Appl. Phys. Lett.* **94,** 021117 (2009).
27. Yeh, K.-L., Hoffmann, M. C., Hebling, J. & Nelson, K. A. Generation of 10 μJ ultrashort terahertz pulses by optical rectification. *Appl. Phys. Lett.* **90,** 171121 (2007).
28. Ammosov, M. V., Delone, N. B. & Krainov, V. P. Tunnelling ionization of complex atoms and of atomic ions in an alternating electromagnetic field. *Sov. Phys. JETP* **64,** 1191–1194 (1986).
29. McDaniel, E. W. *Collision Phenomena in Ionized Gases* (John Wiley & Sons, 1964).
30. Mlejnek, M., Wright, E. M. & Moleney, J. V. Moving-focus versus self-waveguiding model for long-distance propagation of femtosecond pulses in air. *IEEE J. Quantum. Electron.* **35,** 1771–1776 (1999).

Acknowledgements

The authors thank N. Karpowicz for technical assistance and scientific discussions. We also gratefully acknowledge support from the National Science Foundation, Defense Threat Reduction Agency and the Department of Homeland Security through the DHS-ALERT Center under award no. 2008-ST-061-ED0001. The views and conclusions contained in this document are those of the authors and should not be interpreted as necessarily representing the official policies, either expressed or implied, of the U.S. Department of Homeland Security.

Author contributions

J.L. designed the experiment and performed the simulation. J.D. designed the phase compensator and performed remote terahertz sensing. X.-C.Z. and S.L.C. provided theoretical analysis and guidance. X.-C.Z. initiated and supervised the project. All authors contributed to the final manuscript.

Additional information

The authors declare no competing financial interests. Supplementary information accompanies this paper at www.nature.com/naturephotonics. Reprints and permission information is available online at http://npg.nature.com/reprintsandpermissions/. Correspondence and requests for materials should be addressed to X.C.Z.